Transient Analysis of Hybrid Rocket Combustion by the Zeldovich-Novozhilov Method

Changjin Lee*, Jae-Woo Lee, Do-Young Byun
Department of Aerospace Engineering, Konkuk University, #1 Hwayang-dong, Kwangjin-gu, Seoul 143-701, Korea

Hybrid rocket combustion has a manifestation of stable response to the perturbations compared to solid propellant combustion. Recently, it has revealed that the low frequency combustion instability about 10 Hz was occurred mainly due to thermal inertia of solid fuel. In this paper, the combustion response function was theoretically derived by use of ZN(Zeldovich-Novozhilov) method. The result with HTPB/LOX combination showed a quite good agreement in response function with previous works and could predict the low frequency oscillations with a peak around 10 Hz which was observed experimentally. Also, it was found that the amplification region in the frequency domain is independent of the regression rate exponent n but showed the dependence of activation energy. Moreover, the response function has shown that the hybrid combustion system was stable due to negative heat release of solid fuel for vaporization, even though the addition of energetic ingredients such as AP and Al could lead to increase heat release at the fuel surface.

Key Words : Hybrid Rocket Combustion, Zeldovich-Novozhilov Method, Combustion Instability, Negative Heat Release, Thermal Inertia of Solid Fuel

Nomenclature

a : Regression rate constant
c : Specific heat of solid fuel
E_a : Activation energy
f : Temperature gradient at surface
G_{ox} : Oxidizer mass flux
k : Thermal conductivity
n : Regression rate exponent
Q_c : Heat release by decomposition
r : Regression rate
R : Non-dimensional regression rate
R_{Gox} : Response function to oxidizer mass flux fluctuation
R_u : Universal gas constant
T : Temperature
x : X-axis
X : Non-dimensional x-axis
α_s : Thermal diffusivity of solid fuel
α : Roots of $\alpha(\alpha-1)=i\Omega$
κ : Sensitivity parameter
ρ : Density
ε : Non-dimensional activation energy
ν : Sensitivity parameter defined in (13)
Ω : Non-dimensional frequency
τ : Non-dimensional time
μ : Sensitivity parameter defined in (13)
θ : Non-dimensional temperature
π : Sensitivity parameter defined in (13)
ω : Dimensional angular frequency

Subscripts and superscripts

$(\ )_c$: Condensed phase
$\bar{(\ )}$: Steady state
$\hat{(\ )}$: Function of x only
$(\ )_s$: Surface
$(\ )'$: Perturbed quantity
$(\ )_o$: Cold boundary of fuel

* Corresponding Author.
E-mail : cjlee@konkuk.ac.kr
TEL : +82-2-450-3533; **FAX** : +82-2-444-6670
Department of Aerospace Engineering, Konkuk University, #1 Hwayang-dong, Kwangjin-gu, Seoul 143-701, Korea. (Manuscript **Received** January 29, 2003; **Revised** June 23, 2003)

$( )_{ox}$: Oxidizer

1. Introduction

Hybrid rocket has regained a spotlight not only by its excellent safety in combustion process but also by its advantage in development cost although the inferiority of density specific impulse and the low charging efficiency. Generally, hybrid rocket combustion is very complicated by interaction between the solid fuel regression rate and the heat transfer from the boundary layer of chemically reacting flow. The combustion is basically the turbulent diffusion flame, for which the flame is formed by diffusion of oxidizer and vaporized fuel gas within the boundary layer. Many experimental results reported that the unbounded pressure oscillations usually found in solid and liquid rocket systems have not been observed in hybrid motors.

Two types of combustion instability have been shown in the hybrid rocket tests. One of them is the instability induced by an oxidizer feeding system and the other is the flame holding instability due to acoustic disturbances in a re-circulation zone. Jenkins and Cook (1995) had focused on low frequency oscillation around 10 Hz with theoretical model of 1-D hybrid rocket. They specially concerned about fill time of oxidizer flux in the motor as the candidate of low frequency oscillations and studied L^* dependency on the frequency of oscillation. And their study did show a quite good agreement with experimental data observed various tests.

Recently, Karabeyglu and Altman (1997, 1999) had identified that low frequency oscillations in hybrid rocket combustion are mainly due to both thermal lag of solid fuel and the boundary layer adjustment to external perturbations. They also explored the instability mechanism by the use of linear perturbation method as an interaction between the regression rate with the heat flux through the boundary layer and the thermal diffusion of solid fuel.

Rocker (2000) had conducted a series of experimental tests with 24 inch hybrid motor to identify and to simulate the non-acoustic low frequency instabilities. In the results, he found three types of oscillation with different frequency ranges; 2~3 Hz, 6.5 Hz and around 10 Hz. The process of fill-flush of oxidizer in the grain may induce 2~3 Hz oscillation and 6.5 Hz oscillation was found to be attributed to the feed system vibration.

Although many researches have revealed the fundamental mechanism of low frequency oscillations around 10 Hz in hybrid rocket system, it is also true that many aspects of instability still remains unveiled. For example, the result by Karabeyglu and Altman (1997, 1999) did not reveal the effect of some operating parameters on the stability behavior such as surface temperature of solid fuel and heat release by decomposition. In this study, therefore, low frequency instability about 10 Hz is mainly focused for the linear analysis by the use of ZN(Zeldovich-Novozhilov) method, which was successfully applied to the stability analysis of solid propellant combustion (Nobozhilov, 1992; Lee and Kim, 1999). Unlike the previous studies (Karabeyglu and Altman, 1997, 1999), thermal inertia of solid fuel was only accounted for in the analysis and the response function of regression rate to the oxidizer flux perturbations was directly derived. The effect of the regression rate exponent n on the combustion instability was examined. Also the stability behavior of combustion was checked with the change of sensitivity parameters. Then, we tried to explain the basic mechanism of low frequency instability and the characteristics of intrinsic instability of hybrid rocket motor.

2. Governing Equations

Schematic of solid fuel and oxidizer flux is shown in Fig 1. Solid fuel was assumed to move vertically with the regression rate r, so the surface remains unchanged. By assuming the quasi-steady response in the gas phase, the unsteady energy equation of solid fuel is the only equation needed for low-frequency instability of hybrid motor. In the energy equation, the heat needed for decomposition, pyrolysis and vaporization was assumed negligible compared to the total amount of heat transferred to fuel surface. The governing

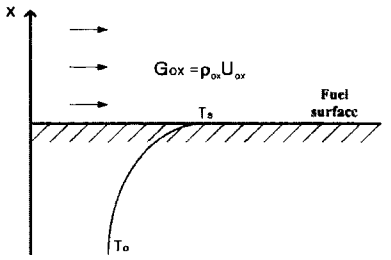

Fig. 1 Schematic of 2-D solid fuel surface and reference coordinate

equation is, therefore,

$$\rho_c c_c \left(\frac{\partial T}{\partial t}+r\frac{\partial T}{\partial x}\right)=k_c\frac{\partial^2 T}{\partial x^2} \tag{1-a}$$

And boundary conditions are

$$\begin{aligned} x&\rightarrow-\infty \quad T=T_o \\ x&=0 \quad\quad T=T_s \end{aligned} \tag{1-b}$$

It should be noted that the surface temperature T_s, which is still unknown, was used in the boundary condition even though the surface temperature should be determined by the heat balance between heat conduction through solid fuel and convective heat transfer from hot gas region. However, Karbeyglu and Altman (1997, 1999) used a heat balance condition at surface instead. Non-dimensional parameters were adopted to transform the governing equation into non-dimensional one. Then the equation becomes

$$\frac{\partial\theta}{\partial\tau}+R\frac{\partial\theta}{\partial X}=\frac{\partial^2\theta}{\partial X^2} \tag{2-a}$$

Here

$$\begin{aligned} &\theta=\frac{T-T_0}{\bar{T}_s-T_0},\ X=\frac{x}{\alpha_s/\bar{r}},\ \tau=\frac{t}{\alpha_s/\bar{r}^2} \\ &R=r/\bar{r},\ \phi=f/\bar{f},\ f=\left(\frac{\partial T}{\partial x}\right)_0 \end{aligned} \tag{2-b}$$

$(\bar{\ })$ means a steady state variable and α_s a thermal diffusivity of solid fuel. Since the perturbation takes place based on the steady state combustion, it is reasonable to obtain the steady solution of the energy equation first. And the steady equation becomes

$$R\frac{\partial\bar{\theta}}{\partial X}=\frac{\partial^2\bar{\theta}}{\partial X^2} \tag{3}$$

with boundary conditions

$$\begin{aligned} X&\rightarrow-\infty \quad \bar{\theta}=0 \\ X&=0 \quad\quad \bar{\theta}=1 \end{aligned}$$

And the steady solution with $\bar{R}=1$ has a form

$$\bar{\theta}(X)=\exp(X) \tag{4}$$

In the linear analysis, perturbations of non-dimensional regression rate R and non-dimensional temperature θ can be assumed as the sum of steady value and Fourier perturbed function respectively as

$$\begin{aligned} R&=1+\hat{R}e^{i\Omega\tau} \\ \theta&=\bar{\theta}+\hat{\theta}(X)\,e^{i\Omega\tau} \end{aligned} \tag{5}$$

Thus, the perturbed governing equation becomes

$$\frac{\partial^2\hat{\theta}}{\partial X^2}+\frac{\partial\hat{\theta}}{\partial X}-i\Omega\hat{\theta}=\hat{R}e^X \tag{6}$$

And the perturbed temperature in the solid fuel is

$$\hat{\theta}(X)=c_1e^{\alpha X}-\frac{1}{i\Omega}\hat{R}e^X \tag{7}$$

Here c_1 is an integration constant, $\alpha(\alpha-1)=i\Omega$, and i is an imaginary number; $i^2=-1$. And a dimensionless angular frequency is denoted by Ω and has the relation with dimensional frequency as $\Omega=\omega(\alpha_s/\bar{r}^2)$. Since this derivation was basically the same as that by Novozhilov (1992) and, Ibiricu and Williams (1975).

3. Response Function

In the previous studies, the stability analysis included two kinds of combustion response; the response of turbulent boundary layer to the oxidizer fluctuation and the response of thermal inertia to heat transfer fluctuation to the fuel surface. According to previous results, time for boundary layer adjustment was found as an order of 100 ms ranging from 40 ms to 160 ms depending on various motor sizes, which is comparable to thermal lag time scale (~178 ms). Thus it is plausible to assume the boundary layer adjustment time cannot significantly affect the fundamental frequency of the system since the frequency is approximately proportional to the inverse of characteristic time. In this study, therefore, it was assumed that the boundary layer

adjustment to the oxidizer perturbation completed instantaneously. Also, the thermal inertia of solid fuel was considered as a dominant factor to cause low frequency oscillations.

It is possible to assume that the instantaneous regression rate r and the surface temperature T_s depends on the temperature gradient at the surface and oxidizer mass flux as

$$T_s=T_s(f,\ G_{ox}) \qquad r=r(f,\ G_{ox}) \tag{8}$$

This is the main idea of ZN method originally adopted by Novozhilov (1992) for the stability analysis of solid propellant combustion. As seen in Eq. (8), surface temperature and regression rate is linked indirectly with heat transfer fluctuations from the hot gas region respectively. This relation is valid in hybrid system regardless of the type of burning regime, unsteady or quasi-steady. Also the effective temperature T_e can be defined by the steady solution of energy equation at the surface as

$$T_e=\bar{T}_s-\frac{a_s}{\bar{r}}f \tag{9}$$

Combining Eqs. (8) and (9), the functional dependency of T_s and r can be finally derived as

$$T_s=T_s(T_e,\ G_{ox}) \qquad r=r(T_e,\ G_{ox}) \tag{10}$$

Thus, it is not difficult to obtain the combustion response function to oxidizer flux fluctuation without having detailed characteristics of heat transfer from the hot gas region. It is well known the regression rate r of hybrid motor has the functional relation with oxidizer mass flux that is analogous to the burning rate in the solid motor as $r=aG_{ox}^n$. Here G_{ox} is the oxidizer flux in the grain of hybrid rocket motor and the constants a, n can be experimentally determined.

During the oxidizer mass flux fluctuations, G_{ox} is perturbed from the steady value. Also, it is appropriate to represent the unsteady regression rate and the surface temperature as the sum of steady value and the small corrections accounting for only the first order derivative as shown in Eq. (5), if the burning surface is weakly perturbed by the oxidizer flux fluctuation. Also, we have a perturbed regression rate and a perturbed surface temperature in the mathematically exact form without resorting to the detail in the gas phase.

$$\begin{aligned} dT_s&=\left(\frac{\partial T_s}{\partial T_o}\right)dT_o+\left(\frac{\partial T_s}{\partial G_{ox}}\right)dG_{ox}\\ dr&=\left(\frac{\partial r}{\partial T_o}\right)dT_o+\left(\frac{\partial r}{\partial G_{ox}}\right)dG_{ox}\end{aligned} \tag{11}$$

The non-dimensional form of the exact relations in Eq. (11) become respectively

$$\begin{aligned} \hat{\theta}_s&=(\hat{\theta}_s-\hat{\phi}+\hat{R})\,\pi+\mu\hat{G}\\ \hat{R}&=(\hat{\theta}_s-\hat{\phi}+\hat{R})\,\kappa+\nu\hat{G}\end{aligned} \tag{12}$$

Here $\hat{G}=G'_{ox}/\bar{G}_{ox}$ and sensitive parameters are defined by

$$\begin{aligned} &\kappa=(\bar{T}_s-T_o)\left(\frac{\partial \ln \bar{r}}{\partial T_o}\right),\ \pi=\left(\frac{\partial \bar{T}_s}{\partial T_o}\right)\\ &\nu=\left(\frac{\partial \ln \bar{r}}{\partial \ln \bar{G}_{ox}}\right),\ \mu=\frac{1}{\bar{T}_s-T_o}\left(\frac{\partial \ln \bar{T}_s}{\partial \ln \bar{G}_{ox}}\right)\\ &\delta=\nu\pi-\mu\kappa\end{aligned} \tag{13}$$

The response function is defined by the ratio of normalized regression rate perturbation to the normalized oxidizer mass flux fluctuation and it becomes as

$$R_{Gox}=\frac{\hat{R}}{\hat{G}}=\frac{(r'/\bar{r})}{G'_{ox}/\bar{G}_{ox}} \tag{14}$$

It is not difficult to find that two more independent relations are required to eliminate $\hat{\phi}$ and $\hat{\theta}_s$ and to derive the response function from Eq. (12). By the use of perturbed temperature and the perturbed temperature gradient at the surface, the response function becomes

$$R_{Gox}=\frac{\nu+\delta(\alpha-1)}{1+(\pi-\kappa/\alpha)(\alpha-1)} \tag{15}$$

This represents the response of the regression rate to the oxidizer flux perturbations. Thus, the response of hybrid rocket combustion can be analyzed by the response function. Here Jacobian δ is chosen as zero since the regression rate r and surface temperature T_s shows a certain correlation with each other. Also it is instructive to note the steady value of the response function R_{Gox} becomes n, the regression rate exponent, in the limit of $\Omega\rightarrow 0$.

Sensitivity parameters π and κ are very important factors in determining the intrinsic stability

behavior of response function. By reviewing the response function $R_{G_{ox}}$ and setting the denominator to be zero, it is possible to derive the intrinsic instability condition that renders the combustion response unbounded. Novozhilov (1992) studied the intrinsic stability and identified the stable region in (κ, π) plane. The simple manipulation revealed the sensitivity parameter should be in the certain range as $0<\pi<1$, $\kappa>1$ for stable response to the external perturbations. Thus, the stability region is defined as

$$\kappa<1 \text{ always stable}$$
$$\kappa>1 \text{ stable only if } \quad \pi>\frac{(\kappa-1)^2}{\kappa+1}$$

The combustion shows always a stable response if sensitivity parameter of (κ, π) remains inside of the boundary. However, the response function becomes unbounded as the point in (κ, π) plane approaches the boundary. It is, therefore, true that the closer to the boundary, the larger the amplitude of the response function. The outside of the boundary corresponds to the region of unstable response. This is quite analogous to the mathematical concept of resonance for spring-mass system with the presence of an external excitation. The thick solid line in Fig. 8 shows the stability boundary.

Asymptotic expression of regression rate

For solid propellant combustion, Ibiricu and Williams (1975) proposed an asymptotic expression of burning rate in the steady state. The burning rate has the form

$$(\rho_s r)^2=\frac{\bar{A}R_u\bar{T}_s^2\rho_s^2 c\alpha_s \exp(-E_a/R_u\bar{T}_s)}{E_a[c(\bar{T}_s-T_0)-Q_c/2]} \quad (16)$$

Although the expression for regression rate is valid only for steady state combustion, we assume that this expression can be applicable to the combustion environment where the perturbations are sufficiently small compared to steady operational state. Here Q_c represents the heat release by decomposition of solid fuel at the surface. Also the chemical reaction is assumed to obey Arrhenius's law; $r=\bar{A}\rho_s \exp(-E_a/R_u\bar{T}_s)$. It is, however, to note that solid fuel does not generate any heat release during decomposition. Moreover, solid fuel needs heat fluxes from the hot gas region for gasification and decomposition is endothermic reaction of the order of magnitude of 300~400 cal/gr. Here $\bar{A}$ is the pre-exponential factor, c is specific heat, and E_a is activation energy of solid fuel. By using the regression rate expression, sensitivity parameters and non-dimensional activation energy ε can be defined as

$$\varepsilon=\frac{E_a}{R_u\bar{T}_s^2}(\bar{T}_s-T_o),\ \nu=\left(\frac{\partial \ln \bar{r}}{\partial \ln \bar{G}_{ox}}\right)=n$$
$$\kappa=\frac{1}{2}\left[\frac{Q_c}{2C(\bar{T}_s-T_o)}\right]^{-1} \quad (17)$$
$$\pi=\left[\left(\bar{T}_s-T_o-\frac{Q_c}{2C}\right)\left(\frac{2}{\bar{T}_s}+\frac{E_a}{R_u\bar{T}_s^2}\right)-1\right]^{-1}$$

As seen in Eq. (17), sensitivity parameters κ and π depends on several factors such as temperature difference, $\bar{T}_s-T_o$ heat release at the surface Q_c, and non-dimensional activation energy ε. Parameter ν represents the dependence of the regression rate on oxidizer mass flux and identically equals to the regression rate exponent n as shown in Eq. (17). It is very instructive to note that the stability behavior of (κ, π) corresponding to the change of operating parameters can take an important role in determining the combustion stability.

4. Results and Discussion

It is well known that the regression rate r is dependent on the oxidizer mass flux and has a form of

$$r=aG_{ox}^n \quad (18)$$

The nominal range of the regression rate exponent n is between 0.4 and 0.9 for HTPB fuel, although the addition of Al or AP (Ammonium Perchlorate) leads to increase in the exponent up to 0.96. (Ibincu and Williams, 1975) In this study, the response function was studied only for HTPB/LOX hybrid system. The material properties of HTPB are mainly excerpted from Karabeyglu and Altman (1997, 1999). The nominal and material properties are specified as follows; specific heat $c=0.57$ cal/gr K, density

$\rho_s=0.93$ gr/cm^3, thermal diffusivity $\alpha_s=1.0\times 10^{-3}$ cm^2/sec, and surface temperature $T_s=820$ K. The temperature at the cold boundary was assumed $T_0=300$ K. In the calculation, the reference regression rate was also used as 0.075 cm/sec. Using the material properties, the thermal lag time was calculated as $\tau_{th}=\alpha_s/r^2=0.178$ sec, which represented that the solid fuel system had an intrinsic frequency of about 5~10 Hz to perturbations. The variety of the exponent in the range of $n=0.5\sim0.9$ was also used. The activation energy of solid fuel, HTPB, was selected in the range of $E_a=12\sim60$ kcal/mole, and the corresponding non-dimensional activation energy ε was between 4.7 and 23.4.

Figure 2 shows the combustion responses to oxidizer fluctuations for $n=0.5$ and $n=0.8$ respectively. Heat release was assumed to be zero for the purpose of simplification in this calculation. As can be seen, three response curves are displayed with the change of non-dimensional activation energy from 10 to 30 for each regression exponent n. The limiting value of the response function R_{Gox} becomes ν when non-dimensional frequency Ω approaches to zero, and we know that the amplitude of steady state response, ν, was identified as the regression rate exponent n from Eq. (17). For $n=0.5$, the response curve shows its peak frequency at around 4 Hz when $\varepsilon=10$. It is not difficult to observe the peak frequency migrates to 8 Hz and 11 Hz as non-dimensional activation energy ε increases up to 30. For $n=0.8$, the response curves show the similarity in shape and pattern to the response curves for $n=0.5$ except for the amplitude of the response. The amplitude of response function seems to be quite dependent on the exponent n and shows a larger peak for a larger n. In addition, the location of peak frequency migrates to a higher frequency as non-dimensional activation energy ε becomes large with a similar peak frequency pattern as shown in the response curve for $n=0.5$. The exponent n, however, does not influence on migration of peak frequency of response function. Similarity can be seen between two curves for different exponent $n=0.8$, and $n=0.5$. One of the best methods to find the similarity between two curves is the normalization by the initial value.

Figure 3 shows the response curves normalized by the steady amplitude of response function, n, which is equivalent to the amplitude of response function in the limit of $\Omega\rightarrow 0$. Also it is interesting to find that response curves show the similarity in shape regardless of the exponent n and only depend on the non-dimensional activation energy ε. In the actual system, the exponent n represents the combustion characteristics of solid fuel and is generally in the range of $0.4<n<0.9$. There

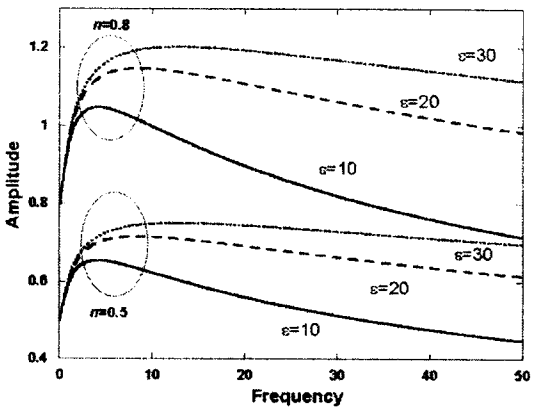

Fig. 2 Response curves for $n=0.5$, and $n=0.8$ with various activation energy. Similarity can be found in response curves for different n

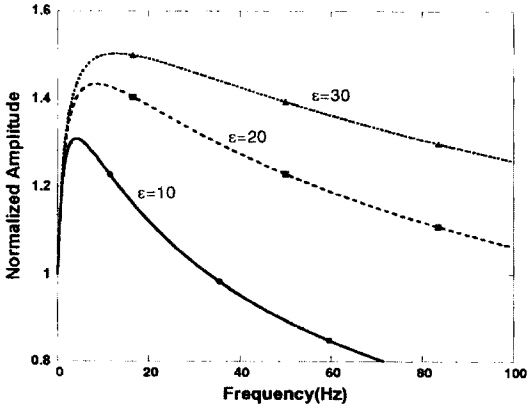

Fig. 3 Normalized response curves with various values of activation energy. The regression rate exponent n does not have an influence on the response curve

should be an influence of n on the response behavior of the combustion. However, this study with a linear analysis could not reveal the influence of the exponent n on the combustion response and will be remained as a future research topic.

It should be also noted that the influence of heat release by decomposition Q_c on the response does not accounted for in Fig. 3. Since the amplitude of response function was normalized by the steady state response n, the normalized amplitude above unity denotes the region of the amplification of input perturbations. As can be seen in Fig. 3, the increase in the activation energy ε enlarges the amplification region in the frequency domain. Also, the peak frequency was observed to move toward a higher frequency from 4 Hz for $\varepsilon=10$ to 12 Hz for $\varepsilon=30$. This result for HTPB hybrid system shows a quite good agreement with the previous result in Karabeyglu and Altman (1999). The thermal lag time of HTPB/LOX system was evaluated $\tau_{th}=\alpha_s/r^2=0.178$ sec based on the material properties at the nominal condition in this study. As can be seen in Fig. 3, thermal lag time of the system did not have any influence on the behavior of response function. Although Karabeyglu and Altman claimed that the system with a smaller thermal relaxation time would have a broader frequency range of amplification (Karabeyglu and Altman, 1999), the current study found that the dominant factor in determining the response shape is not the thermal relaxation time but the activation energy.

Figure 4 shows three curves normalized by the amplitude of steady state n that show the influence of heat release Q_c on the response function at the nominal conditions when activation energy ε is 10. The solid fuel in hybrid rocket, HTPB, needs the latent heat flux for vaporization of order of 300~400 cal/gr since no oxidizer is included in the composition whereas the solid propellant such as HTPB/AP/Al generates a substantial amount of heat of order of 100 cal/gr during decomposition at the surface. Thus, it is interesting to find the effect of Q_c on the behavior of response function with other parameters fixed. As seen in Fig. 4, three values of heat release Q_c of -100, 0 and 100 cal/gr are used in the calculation. The amplitude of response function for $Q_c=100$ cal/gr is much larger than that for the negative heat release, although the location of peak frequency is about 4 Hz, and the regions of amplification are also qualitatively the same for all case of Q_c. Thus, we can find the increase in Q_c causes the combustion response to have a larger amplitude and consequently to be more sensitive. Although the negative heat release Q_c that is true for hybrid rocket motor leads the response to be more stable to external perturbations. Thus, the negative heat release, the latent heat for vaporization, can be regarded as one of the factor for hybrid rocket motor to have the stable combustion response.

Another aspect to be considered is the stability behavior of sensitivity parameters in (κ, π) plane. As mentioned in the previous section, sensitivity parameters κ and π take an important role in determining the stability behavior of response function. The change of operating parameters such as activation energy, surface temperature, and heat release can influence on the sensitivity parameters κ and π. Also the corresponding variation of sensitivity parameters forms a trajectory in (κ, π) plane. Thus, the stability behavior of response function can be determined simply by

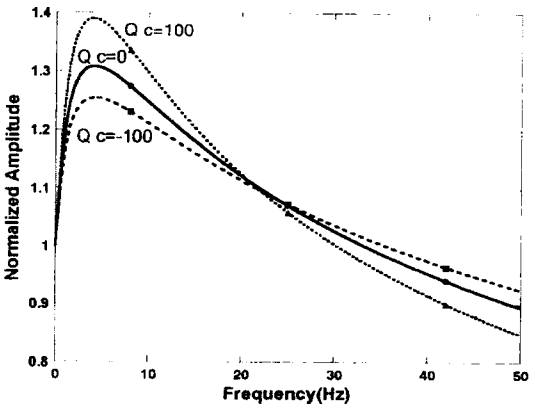

Fig. 4 Normalized response curves for various heat release Q_c. The location of peak frequency remains unchanged at about 4 Hz for all cases of heat release

monitoring the trajectory in (κ, π) plane. If the trajectory moves toward the stability boundary, the amplitude of the response becomes larger and combustion response becomes more sensitive to external perturbations. The response leads to instability if the trajectory crosses over the boundary.

In the next, the parametric study was done to find the influence of activation energy ε, and $\bar{T}_s - T_o$ on the stability behavior in the intrinsic stability plane. Shown in Eq. (17), the parameter κ is dependent upon the heat release Q_c and $\bar{T}_s - T_o$. The sensitivity parameter π is a function of an activation energy E_a, heat release Q_c and $\bar{T}_s - T_o$. The influence of Q_c on κ is shown in Fig. 5 against various values of $\bar{T}_s - T_o$ of 350, 450, and 520. The activation energy is 20 Kcal/mole in the calculation. The parameter κ shows a monotonic increase for a fixed $\bar{T}_s - T_o$ as heat release Q_c increases. However, the increasing rate of κ diminishes as $\bar{T}_s - T_o$ increases and a very steep increase of κ is found around when heat release Q_c becomes 300 and is $\bar{T}_s - T_o$ 350. However, sensitivity parameter κ does not change too much regardless of the change of $\bar{T}_s - T_o$ and shows a monotonic decrease from 0.5 as long as heat release Q_c remains negative. Thus, we can see the negative heat release Q_c leads the sensitivity parameter κ to decrease monotonically for all cases of $\bar{T}_s - T_o$ and the trajectory of κ moves consequently toward inside of the stability boundary in (κ, π) plane. This can explain how the negative heat release of solid fuel contributes to stabilize the combustion response of hybrid rocket motor.

Similarly as shown in Fig. 5, the change of sensitivity parameter π can be found in Fig. 6 as heat release Q_c increases for three cases of $\bar{T}_s - T_o = 350$, 450, and 520. In the calculation, nondimensional activation energy ε is fixed as 5. Sensitivity parameter π shows a monotonic increase as heat release Q_c increases and followed by a steep increase to infinity for all cases of $\bar{T}_s - T_o$. Also the change in for the case of $\bar{T}_s - T_o = 350$ shows a faster rise than other cases with larger $\bar{T}_s - T_o$. However, π falls into one curve as Q_c becomes negative and approaches to 0.18 for all cases of $\bar{T}_s - T_o$. Thus, we can see that sensitivity parameter π does not depend on $\bar{T}_s - T_o$ when Q_c is negative. It should be noted that a parameter π is physically limited within the range between zero and unity. Also details can be found in reference by George and Krishnan (1998).

Figure 7 is a graph showing the effect of nondimensional activation energy ε on the change of π with a fixed $\bar{T}_s - T_o = 350$ as heat release

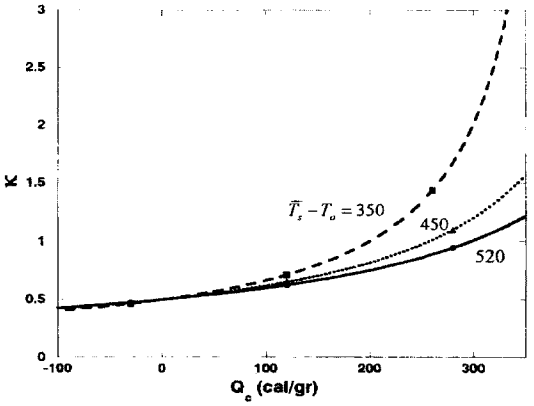

Fig. 5 The influence of heat release Q_c on the sensitivity parameter κ for various $\bar{T}_s - T_o$ with a fixed ε. Sensitivity parameter κ does not change too much for different $\bar{T}_s - T_o$ when heat release Q_c is negative

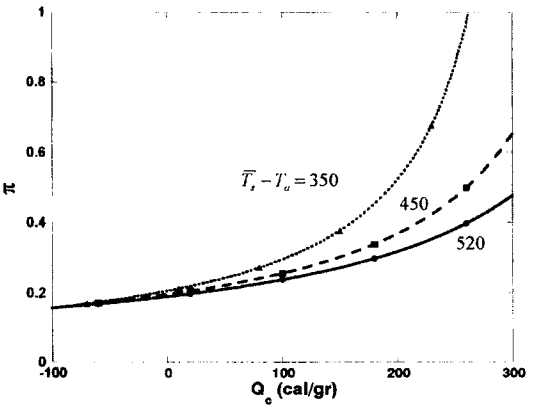

Fig. 6 Effect of heat release Q_c on the sensitivity parameter π for various $\bar{T}_s - T_o$ with a fixed ε. While heat release is negative, π becomes one value for all $\bar{T}_s - T_o$

Q_c increases. Non-dimensional activation energy ε is selected as 5, 10 and 20 respectively. As seen in Fig. 7, each curve for a fixed ε increases monotonically and followed by rapid rise and shows a very similar increase pattern. The big difference from curves is the point where it shows a rapid rise to infinity. For example, π becomes almost infinity at about $Q_c=300$ when ε is 20. Whereas, we can see the steep increase at about $Q_c=120$ when ε is 5. The absolute value of π for a large ε is much less than that for a small ε over all Q_c. So, we can say sensitivity parameter π is relatively insensitive to the change of Q_c. Also π remains small for large activation energy. The result shows that the change of heat release Q_c, the temperature difference $\bar{T}_s-T_o$, and/or the activation energy ε may change the characteristics of intrinsic stability of hybrid combustion system by altering the parameter π. We can conclude that sensitivity parameter π remains small and does not alter too much while Q_c is negative and also insensitive to the change of $\bar{T}_s-T_o$ and ε.

As previously mentioned, operating parameters such as heat release Q_c, $\bar{T}_s-T_o$ and ε can change sensitivity parameters κ and π simultaneously in forming a trajectory in (κ, π) plane. Figure 8 shows the intrinsic stability boundary of thermal lag system and two trajectories of (κ, π) with change of operating parameters. A thick line in Fig. 8 denotes the intrinsic stability boundary. The stable region is, then, the left of the boundary. The starting point of a trajectory A is a point (0.5, 0.168) in (κ, π) plane when heat release Q_c is zero, and $\bar{T}_s-T_o=520$. The direction of a trajectory A is the direction of increase in heat release Q_c up to 350 cal/gr. Here non-dimensional activation energy is fixed as 7.8. As seen in Fig. 8, the trajectory A remains inside of stable region as heat release Q_c increases since the increasing rate in π exceeds that of κ. Thus, we can see that the increase in heat release Q_c does not totally alter the stability behavior of the response function in this case.

However, it is very interesting to see that the decrease in the temperature difference $\bar{T}_s-T_o$ can lead the trajectory B of (κ, π) into the unstable region by crossing the boundary. The starting point of B is (1.204, 0.109) and the heat release Q_c is fixed as 300 cal/gr. Also, the non-dimensional activation energy ε is 19.5, and the surface temperature $\bar{T}_s$ and cold boundary temperature T_o are fixed as 750 K, 300 K respectively in the calculation. As surface temperature decreases from 750 K to 620 K and resulting $\bar{T}_s-T_o$ decreases from 450 to 320, the trajectory B moves toward right side showing a faster increase in κ than in π. Finally the trajectory

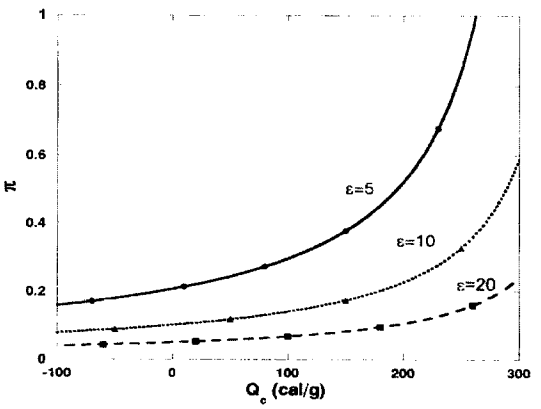

Fig. 7 The influence of heat release Q_c on the sensitivity parameter π for various ε with a fixed $\bar{T}_s-T_o$

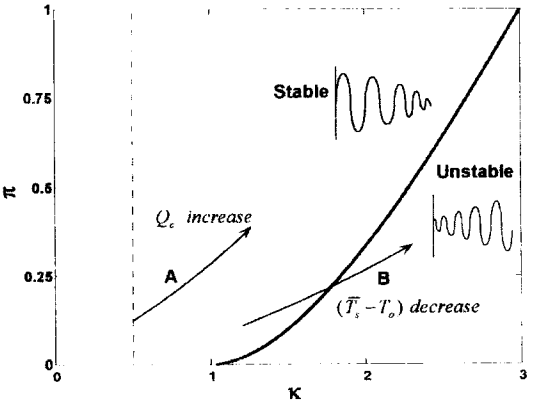

Fig. 8 Boundary of the intrinsic stability and trajectories A and B of (κ, π) as heat release Q_c increases. Trajectory B crosses over the boundary and shows a unconditional instability with the decrease of $\bar{T}_s-T_o$

B crosses over the stability boundary into the unstable regime. Physically, crossing the boundary means the unconditional amplification of input perturbations. This, therefore, implies that the hybrid rocket combustion system can always have an unstable resonance to perturbations if operating conditions would be in a certain condition with a high Q_c and a low $\bar{T}_s - T_o$. In a real hybrid rocket motor, however, we know heat release is generally negative and cannot be attained as large as 350 cal/gr even though some energetic additives such as AP and Al powder would cause heat release Q_c to increase generally. Thus, it is obvious that the hybrid rocket motor operating at the nominal conditions with HTPB/LOX combination has a stable combustion response to the external perturbations. It is also instructive to note that the trajectory B rotates counterclockwise from the original position, which means the combustion response becomes further stable, as heat release Q_c becomes negative.

5. Summary

In this study, ZN(Zeldovich-Novozhilov) method was successfully applied to the hybrid rocket combustion system. It was assumed that the boundary layer adjustment to the oxidizer flux perturbation was instantaneously completed, and the thermal inertia of solid fuel was only accounted for in the analysis. The result shows a quite good agreement with the previous study (Karabeyglu and Altman, 1997, 1999). The trajectory of sensitivity parameters gives us an overall view of the characteristics of intrinsic instability of response function in (κ, π) plane. The followings can summarize the results

(1) ZN method was successfully applied to the thermal lag system of hybrid rocket combustion and showed a quite good agreement with previous study. The low frequency instability around 4~10 Hz in hybrid rocket motor with HTPB/LOX was revealed mainly due to the thermal inertia of solid fuel. Results also show that the stability behavior response function is found to be independent of the regression rate exponent n and the activation energy can dominantly influence on the amplitude of response function.

(2) Even though the increase in heat release Q_c could alter sensitivity parameters π and κ and corresponding stability behavior, the basic characteristics of stability behavior would remain unchanged and stable. Thus the hybrid combustion system was relatively stable even if a small addition of AP and Al would contribute to increase Q_c.

(3) The intrinsic stability was affected significantly by the change of the activation energy Ea and the temperature difference $\bar{T}_s - T_o$. For example, the trajectory in the stability plane shows the border crossing as $\bar{T}_s - T_o$ decreases for a certain operating condition. However, the operating condition such as $Q_c = 350$ cal/gr and $\bar{T}_s = 320$ K is too unrealistic to occur in the real hybrid rocket motor. Thus, we can conclude that hybrid rocket motor does have a stable combustion response for all real operating conditions from the analysis result. Also, it is found that the addition of energetic materials such as AP and Al powder does not alter the stability characteristics of hybrid rocket combustion. The negative heat release is found as a major factor for hybrid thermal system to have a stable response.

Acknowledgment

This work is supported by the research grant from Konkuk University research fund in 2001.

References

George, P. and Krishnan, S., "Fuel Regression Rate Enhancement Studies in HTPB/Gox Hybrid Rocket Motors," *AIAA paper 98-3188*, 34th AIAA/ASME/SAE/ASEE Joint Propulsion Conference & Exhibit.

Ibiricu, M. M. and Williams, F. A., 1975, "Influence of Externally Applied Thermal Radiation of the Burning Rates of Homogeneous Solid Propellant," *Combustion and Flame*, Vol. 24, pp. 185~198.

Jenkins, R. M. and Cook, J. R., 1995, "A Preliminary Analysis of Low Frequency Pressure

Oscillations in Hybrid Rocket Motors," *AIAA Paper 95-2690.*

Karabeyglu, M. A. and Altman, D., 1999, "Dynamic Modeling of Hybrid Rocket Combustion," *Journal of Propulsion and Power*, Vol. 15, No. 4, pp. 562~571.

Karabeyglu, M. A. and Altman, D., 1997, "Transient Behavior in Hybrid Rocket," *AIAA Paper 97-2937.*

Lee, C. and Kim, S. I., 1999, "Re-examination of the Response Function of Solid Propellant with Radiant Heat Flux," *AIAA Paper 99-0590.*

Marxman, G. A., 1965, "Combustion in the Turbulent Boundary Layer on a Vaporizing Surface," *10th Symp. (International) on Combustion*, pp. 1337~1349.

Novozhilov, B. V., 1992, "Theory of Nonsteady Burning and Combustion Stability of Solid Propellants by the Zeldovich-Novozhilov Method," edited by K. K. Kuo and M. Summerfield, Vol. 143, *Progress in Astronautics and Aeronautics*, AIAA, New York, Chap. 15.

Rocker, M., 2000, "Modeling of Non-acoustic Combustion Instability in Simulations of Hybrid Motor Tests," *NASA/TP-2000-209905.*